Measurement 164 (2020) 108043

Contents lists available at ScienceDirect

Measurement

journal homepage: www.elsevier.com/locate/measurement

Smart frost measurement for anti-disaster intelligent control in greenhouses via embedding IoT and hybrid AI methods

Alejandro Castañeda-Miranda [a], Victor M. Castaño-Meneses [b]

[a] Creativity and Innovation Center 4.0 (CIC 4.0), Universidad Tecnológica de Querétaro, Av. Pie de la Cuesta 2501, Colonia Unidad Nacional, Santiago de Querétaro, Querétaro 76148, Mexico

[b] Centro de Física Aplicada y Tecnología Avanzada (CFATA), Universidad Nacional Autónoma de México, Boulevard Juriquilla 3001, Querétaro 76230, Mexico

ARTICLE INFO

Article history:
Received 12 May 2019
Received in revised form 22 May 2020
Accepted 24 May 2020
Available online 2 June 2020

Keywords:
Smart frost measurement in greenhouses
Anti-frost irrigation
Artificial Neural Network
Fuzzy expert system
Internet-of-things
Hybrid AI methods

ABSTRACT

A novel Agro-industrial IoT (AIIoT) technology and architecture for intelligent frost forecasting in greenhouses via hybrid Artificial Intelligence (AI), is reported. The Internet of Things (IoT) allows the objects interconnection on the physical world using sensors and actuators via the Internet. The smart system was designed and implemented through a climatological station equipped with Artificial Neural Networks (ANN) and a fuzzy associative memory (FAM) for ecological control of the anti-frost disaster irrigation. The ANN forecasts the inside temperature of the greenhouses and the fuzzy control predicts the cropland temperatures for the activation of five output levels of the water pump. The results were compared to a Fourier-statistical analysis of hourly data, showing that the ANN models provide a temperature prediction with effectiveness higher than 90%, as compared to monthly data model. Moreover, results of this process were validated through the determination of the coefficient of variance analysis method (R^2).

1. Introduction

According to reports on ecological disasters by environmental freezing, frost damage is a powerful agent of geomorphic change that forms ice on the internal plant tissue, damaging their cells [27]. This geomorphic change depends on air temperature, relative humidity and cooling depth in farmland, among other environmental conditions [29] and the changes of greenhouse configurations and arrangements can influence the inside microclimate [24], to protect the crop against climatic adversity [15]. Recently, ecosystems designs have followed a clever transformation for increasing and improving the production [16], through Artificial Intelligence (AI) to create smart, self-optimizing industrial equipment and facilities [22] to meet the growing food demand worldwide [10]. The new era will involve the use of smart farming technologies, applications, and solutions to ensure better crops and improve the food production [4]. The agroindustry tendency is to use of sustainable greenhouse production with minimized carbon footprint [20]. The research hypothesis of this present work is that if we can regulate the microclimate environmental on greenhouses from presence of an environmental frost, we can estimate the use of water dispersion system on plastic wrap for freeze the plasticized surface and keep thermal energy of greenhouse [13]. The basic idea consists in the internal heat does not escape due to thermal insulation or thermal capacitance caused by the low plastic porosity at low temperatures [7,14]. A water sprinkler system interacts with the greenhouse wrap forming an ice layer on top the plasticized surface [12,30]. We can thus mitigate the effect of drastic temperature changes on agricultural crops caused by the frost environment external to the greenhouse, which is transformed into an igloo. Accordingly, a smart frost control in greenhouses through neural networks using an intelligent weather station has been reported [3] and a Fourier-statistical analysis of hourly data for predict humidity and temperature [2] has been presented [28,6,11,23]. Furthermore, the improved stock on IoT cellular communication for remote access without internet consists in the capacity of collected and stored information on a web server. Now, the frost occurs when the air temperature at ground level falls below zero degrees, physically at that point any liquid under normal conditions begins its freezing process [9,19]. Additionally, the thermal conductivity of samples at temperatures near 0 °C was measured for freeze damage estimations in a cold entity [33,31]. Accordingly, humidity and dry cold directly affects the plant tissue, destroying the internal cells and depending on the thermal resistance of crops, can proceed to the cause irreparable damage to cultivation or total destruction of plants [18,19], whereas other typical crops (corn, bean, maguey, among others)

E-mail addresses: alejandro.castaneda@uteq.edu.mx (A. Castañeda-Miranda), vmcastano@unam.mx (V.M. Castaño-Meneses)

https://doi.org/10.1016/j.measurement.2020.108043
0263-2241/

show significant damage with important economic losses (50–80% of total production). Some particular types of disastrous weather phenomenon in central Mexico are black frosts, which have very negative effects for agriculture and using heaters provokes that stems and leaves of frozen crops does not appear [8,26]. Currently, a new solar greenhouse with thermal storage is investigated, the system that uses water solar heating to raise the air temperature on greenhouses during cold winter nights [1,5,17]. However, the main disadvantage of this thermal performance of a solar greenhouse is in the coldest regions, where frost events may occur regularly.

2. Materials and methods

The implementation and the study location of the embedded intelligent system prototype in greenhouses is located in Tulancingo of Bravo, on the Hidalgo State, Mexico, with geographic coordinates: latitude, 20.0836300°, longitude, −98.3633200° in decimal degrees and elevation of 2153.96 m above sea level. In this place, various tomato species are grown and is the entity that contains different variations of the type of earthly climate which presents recurrent black frosts affecting yield. The flowchart of the process is shown on Fig. 1.

2.1. The embedding hardware

The instrumentation process of smart farming is describing as follows, a data base obtains the data from a meteorological station and is sent remotely by an Xbee-Wifi wireless protocol (WRL-12569 of Sparkfun manufacturer). The data captured is modified by a protocol exchanger device, which is constituted by Intel Edison (DEV-13024 of Sparkfun manufacturer) integrated hardware, a Micro SD Card (64 Gb.) and a GSM/GPRS cellular network device (CEL-13120 of Sparkfun manufacturer). The electric power supply of the meteorological station and embedded internet of things system is self-sustaining using renewable energies through solar cells

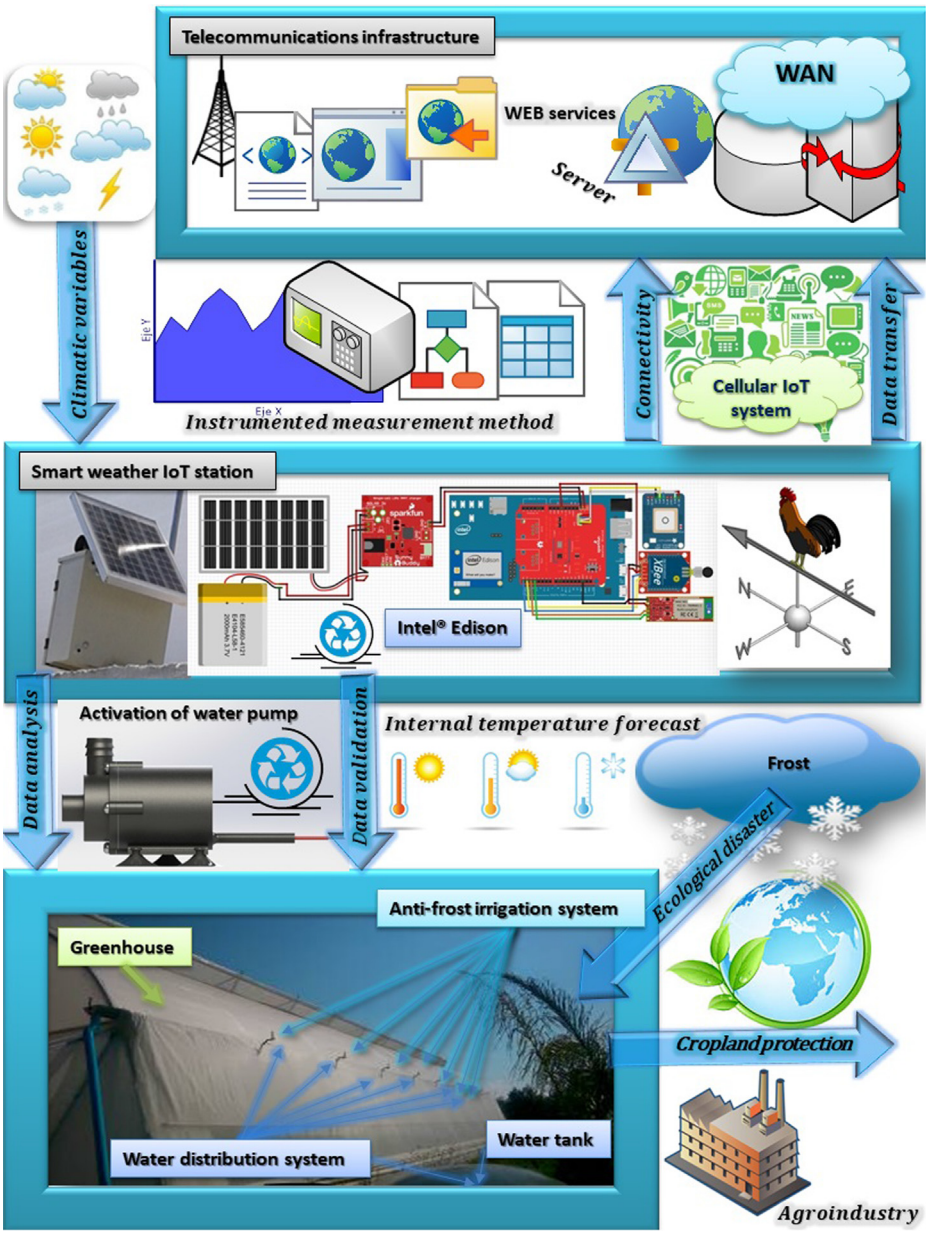

Fig. 1. The process flow diagram for embedded intelligent system prototype applied on greenhouses.

that use a charge controller, a battery power of 12 V to 6 Ah and a DC/DC converter (12 V/5 V). The external remote weather station is implemented using a Weather Shield (DEV-12081 of Sparkfun manufacturer), which data collects using wireless technology information (LMR-12570 of Sparkfun manufacturer) and provides data of barometric pressure, relative humidity, solar radiation and temperature, and also has connections to sensors of wind speed, direction, rain gauge and a GPS for the location (GP635T of Sparkfun manufacturer). Technically, a weather shield contains voltage regulators and signal translators for all devices, where they are integrated to the variables of the weather station with integrated computer platform, which contains an operation menu accessed through a communication of serial port.

2.2. The embedding connectivity

The M2M smart cellular system is characterized by covering greater distances and having more privacy and less vulnerabity than other types of IoT systems, which is ideal for greenhouses that are located in remote or rural areas that are isolated from the urban area. The implementation of software for Internet of Things (IoT) in the integrated system works as follows; the data generated by the weather station is concatenated and sent by a wireless serial protocol. The second part of the intelligent forecasting application consists of implementing the crop protection focused in greenhouses. The intelligent frost irrigation management of the weather phenomenon that transforms in an ecological disaster uses the mathematical models proposed to predict the temperature limits for the frost presence, as shown in Fig. 2.

2.3. The embedding software

The monitoring and control are obtained automatically or manually according to the user's availability through a website, which integrates the different hardware and software solutions (https://www.embeddedcastaneda.com/weather/weather.html).

2.3.1. Methodology for data collection

The data are captured is added by a protocols exchanger. The data is manipulated and stored by an Intel Edison. The integrated system has a Windows IoT operating system. The acquired data is defragmented for use by the syntactic lexicon analyzer implemented on the device. The acquired data is stored on an SD Card using a text file database (*.txt), that is transformed into a Microsoft Excel (*.csv). The data is requested through a Global System for Mobile General and Packet Radio Service (GSM/GPRS) cellular communications, using a Wireless Application Protocol (WAP). Furthermore, that generates a Transmission Control Protocol with Internet Protocol (TCP/IP) using a virtual machine for the subsequent remote connection and the visualization of data to a website.

2.3.2. Methodology for data analysis

The embedded software that is used to analyze data, the database is in Microsoft Excel (*.csv) on an SD card and the programming language was used for data collection is C++ through a host system running a Linux platform and an Intel Edison device is programmed as a neuroprocessor. Thus, the frost prediction in this study uses artificial intelligence, specifically the combination of neural networks and fuzzy systems through a web page. The concept of prediction and behavior of frost involves different factors such as: outdoor air temperature (T_0), relative humidity of outdoor air (R_{h_0}), wind speed (W_s), solar radiation (S_r) and relative humidity of the inner air (R_{h_i}); being the temperature of the air within the variable output (T_i). The temperature of the culture is also incorporated to determine the presence of frost in the form of a fuzzy system.

2.3.3. Methodology for data validation

In addition to the usual quantitative measures such as the mean, mode and standard deviation used to evaluate the performance of a model, the following statistical indices were used to select the best ANN architecture based on the difference between the real and the estimated values. The coefficient of determination (R2) by the percent standard error of the prediction is indicated according to the Eq. (10). For a perfect match, the coefficient of determination (R2) should be close to 1.

$$R^2 = 1 - \left[\sum_{i=1}^{N}\left(y_i - \hat{y}_i\right)^2 / \sum_{i=1}^{N}\left(y_i - \bar{y}_i\right)^2\right] \quad (1)$$

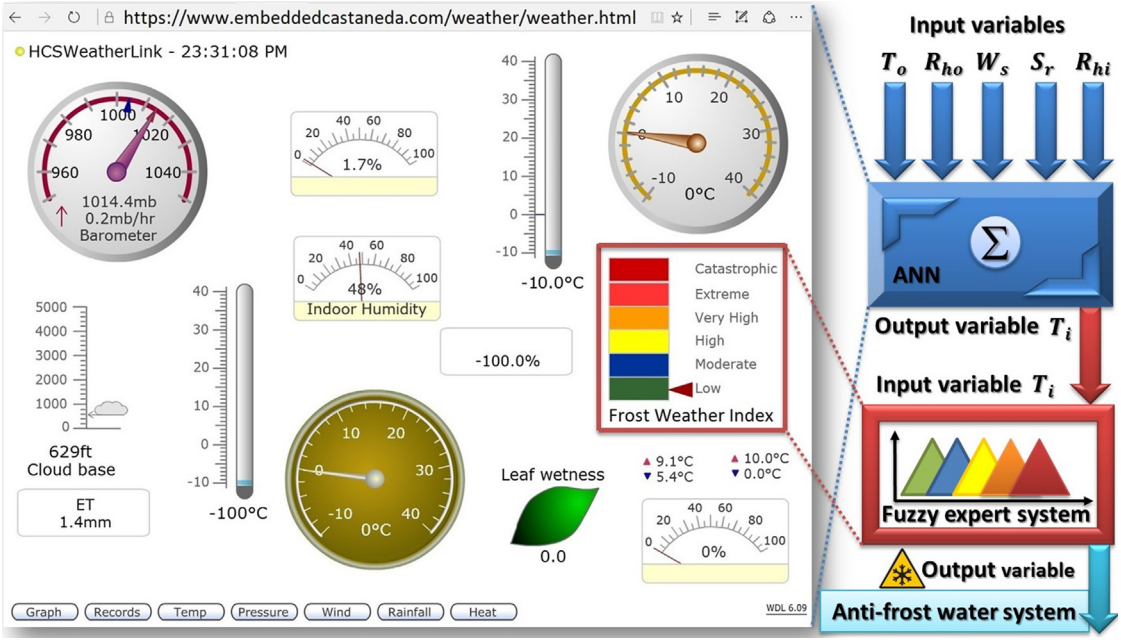

Fig. 2. Block diagram of the anti-frost water system for smart frost prediction.

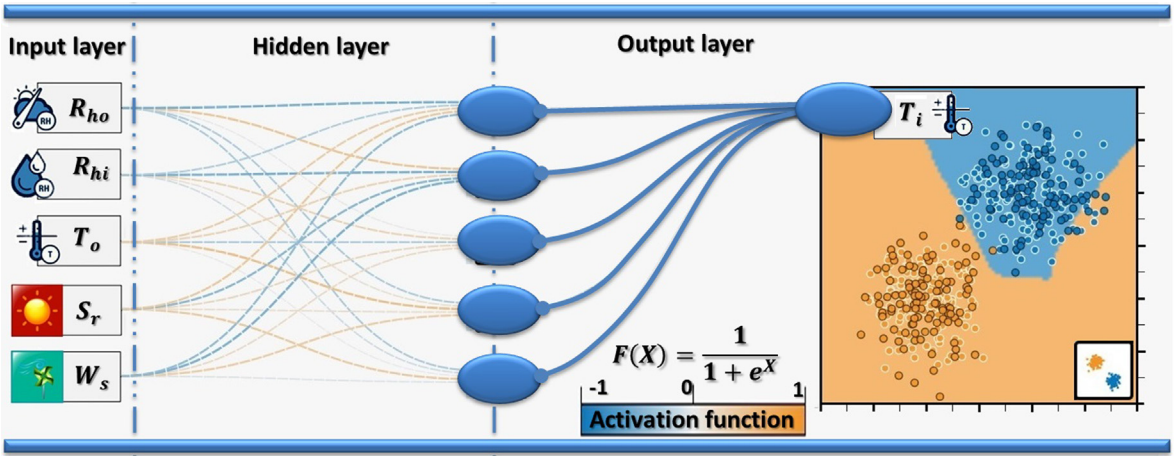

Fig. 3. The flow chart of ANN model uses to predict the interior temperature of greenhouse.

where the estimated value is defined for y_i, the actual value is calculated by $\hat{y}_i$ and the average of actual data set is $\bar{y}_i$, all previous with the consideration of i observations.

3. Theoretical considerations

The adaptive network-based fuzzy inference system (ANFIS) is a kind of artificial neural network that is based on the Takagi–Sugeno fuzzy inference system. In the present method, it is differentiated from ANFIS by the implementation and structure of the fuzzy system, where it considers the inputs of ANN temperature prediction and the cropland temperature, to activate an anti-disaster frost irrigation on the greenhouse plastic surface through a fuzzy controller. The mathematical models proposed are to predict the interior temperature of an greenhouse and the process is based on the analysis of the following input variables: outside air temperature (T_o), outside air relative humidity (R_{ho}), wind speed (W_s), global solar radiation flux (S_r), inside air relative humidity (R_{hi}); being the inside air temperature the output variable (T_i), as shown in the flowchart of Fig. 3. Furthermore, once the temperature has been predicted, the diffuse system is considers activating the ecological anti-disaster irrigation before freezing.

3.1. Artificial Neural Networks (ANN)

In recent years, there has been much research on the Artificial Neural Networks (ANNs). ANNs are algorithms capable of learning from experience based on signals or data from abroad, using a parallel, distributed and adaptive computing framework. The implementation and adaptability to the environment is through software programmed into embedded software devices. These devices present calculation parallelism and distributed memory. According to their definition, ANNs are forecasting tools, due to a mathematical structure capable of describing complex nonlinear relationships between input and output data sets. Therefore, their ability to learn is often defined as a process that optimizes the performance of the network with respect to a given task. ANNs can be considered as algorithms to study and model any given data set. They are a non-standard tool of statistical analysis; through which it is possible to study and make predictions about any data set with ANNs. The propagation rule used consists of linearly combining inputs and synaptic weights. Mathematically, this model is described by:

$$y = F\left(\sum_{i=1}^{N}\sum_{j=1}^{M} \omega_{[jxi]} \cdot x_{[ix1]} + b_{[jx1]}\right) \tag{2}$$

From Eq. (1) a matrix node [jxi] of j neurons per i inputs are defined. Consequently, each neuron of network receives a threshold for$\omega_{[ixj]}$, where $i = 1 \cdots N$ for $j = 1 \cdots M$ neurons. Consider that x is the input vector and $b_{[jx1]}$ is a constant called bias of each neuron and $\omega_{[ixj]}$ is a vector of synaptic weights, F is the sigmoid function of activation [3]:

$$F(X) = 1/(1+e^X) \tag{3}$$

The basic idea of neural networks consists in the learning is a change to the system in order to improve a goal. Suppose we have an objective function $\mathrm{F}(\omega)$, which measures how well a system is currently performing. Nevertheless, the learning is change the synaptic weights, i.e., correspondingly for $\omega \rightarrow \omega + \Delta\omega$. Thus, the change in performances is

$$\Delta\mathrm{F} = \mathrm{F}(\omega + \Delta\omega) - \mathrm{F}(\omega) \tag{4}$$

Then, if we assume that F is smooth, we can estimate ΔF as a function of the gradient of F with respect to ω as follows:

$$\Delta\mathrm{F} = \Delta\omega^{\mathrm{t}} \cdot \nabla_{\omega}\mathrm{F}(\omega) \tag{5}$$

However, if we want to improve performanceF, then $\Delta\mathrm{F} \geq 0$. Moreover, the gradient based algorithms propose that we have to take small step $\Delta\omega$ in the direction of gradient, i.e., the direction of the greatest level of improvement. So, if we take a small step γ, we have the change in performance defined as:

$$\Delta\mathrm{F} = \gamma\nabla_{\mathrm{W}}\mathrm{F}(\mathrm{W})^{\mathrm{t}} \cdot \nabla_{\mathrm{W}}\mathrm{F}(\mathrm{W}) \tag{6}$$

According to this definition, from Eq. (4), that obviously is greater or equal to zero. The training of an ANN is done through a learning algorithm based on the backward propagation (BP) which is a supervised algorithm. This method requires a set of training patterns, and their corresponding desired outputs, and autonomously adjusts the connection weights between the neurons. The correction of the weights is done in accordance with the imposed learning rules and, therefore, obtains a unique knowledge of the data [25].

3.1.1. Artificial neural networks algorithm

This section briefly describes the supervised version of the ANN. The parameter setting of a model used to represent a system is called System Identification. The methods of identifying the system are often classified into two main categories: gray and black box models. Compared to direct modeling, which is governed by the physical laws of the system, these models are adequate to construct a mathematical model where the mechanism of the system is not well understood or where its properties change

unpredictably [21,32]. The gray box methods are a formulation of the model in which the parameters are traceable to real physical principles. The black box method relates the mathematically measured inputs to the measured outputs in which the parameters of the model are transformed without any traditional physical meaning. Black box models do not require prior knowledge of the system, which can be an advantage if the information on the dynamics of the system is limited; however, it involves the problem of selecting a suitable structure for the model. Another advantage of this type of models is the possibility of obtaining a broad model with a relatively small set of measurements. The model can be improved as new data is entered. Compared to a gray box model, the black box approach requires less time and effort to develop. Generally, in a black box model, non-statistical methods or statistical methods are used to formulate the relationship between inputs and outputs. The ANN Model is determined by three factors: (1) the topological structure of the network; (2) neuronal characteristics; and (3) the algorithm of raining. The ANN implemented in this study is a Multilayer Perceptron (MLP) that includes an input layer of 5 nodes, a hidden layer with a variable number of hidden nodes and an output layer that has only one node as shown in the Figs. 2 and 3. Thus, the training of an ANN is done through a procedure called learning algorithm based on the backward propagation (BP) which is a supervised algorithm. This method requires a set of training patterns, and their corresponding desired outputs, and autonomously adjusts the connection weights between the neurons. The training rule for backward propagation between layers is described by Eq. (7), where p layer proceeds to q layer, ΔW_{qp} is the adjustment of synaptic weights between layers, α is a correction increase, E_q is the squared error between the desired responses (r_q) and the current responses (o_q) of the nodes in q layer, n_q is the number of nodes of the q layer and the factor $1/2$ is the product of the error derivative.

$$\Delta W_{qp} = -\alpha\left(\frac{\partial E_Q}{\partial W_{qp}}\right) = -\alpha\left(\frac{1/2\sum_{q=1}^{n_q}(r_q - o_q)^2}{\partial W_{qp}}\right) \tag{7}$$

Hence, to develop an adequate ANN is necessary to work with several iterations, even to solve problems with little complexity, to collect a smaller number of iterations together with the reduction of time in ANN learning. Although used successfully in many real-world applications, the standard backward propagation algorithm (SBP) suffers from a number of shortcomings; one of them is the speed at which the algorithm converges. The reduction of the number of iterations and the acceleration of the learning time of neural networks are topics of recent research; some improvements of the SBP algorithm are the conjugate gradient. Correction of the weights is made according to imposed learning rules and thereby, obtains unique knowledge from the data [3]. One criticism of the ANN model of this reference work is the linearization method, because the attribute vectors lose their discriminant capacity, since the different pattern vectors could originate identical values once the linearization operation is improved. An improvement to this feature avoids the execution of the linear functionality, through the adaptation and implementation of the fuzzy map in the present work. The complexity of the weather during the spring, summer, autumn and winter seasons, using the minimum daily temperature (°C) for different months are shown in the Table 1 and the climatic variables are plotted in the Fig. 4. The modified parameters of ANN in different months of the year are shown in Table 2.

3.2. Fuzzy logic systems

The technique called fuzzy logic allows treating vague and scattered information in terms of fuzzy sets, these allow you to define whether something is included in them by assigning a value between one and zero or is not in a zero the mathematical equation

Table 1
Time complexity using minimum daily temperature (°C) for different months.

Day	Month											
	1	2	3	4	5	6	7	8	9	10	11	12
1	−2	0	−2	4.5	8	8	10	8	10	10	3	4
2	−2	0	−1	7.5	6	8	11	10	7	9	2	1
3	−2	−1	0	5.5	5	8	9	9	8	9	3	0
4	−3	−1	0	4.5	5	10	10	8	8	9	3	0.5
5	−2	−1	6	4	5	9	10	7	8	9	4	0
6	1	4	2	5.5	7	10	10	7	9	9	3.5	−2
7	−2	2.5	0	7	5	10	10	8	9	10	4	−4
8	−2	1	5	5	4	7	11	9	8	10	2	−2
9	−3	−4	3	5.5	8	10	10	9	7	7	3	2.5
10	−1	−1	1	5.5	5	9	10	10	8	8	4	0
11	2	5	0	6	9	9	10	9	9	10	5.5	−2
12	1	−3	4	3	7	10	10	9	9	7	5	−2
13	0	−4	2	8	5	9	10	9	9	7	3	−1
14	−2.5	−1	5	8	5	9	10.5	9	10	6	2	2
15	−0.5	−5.5	0	7	10	7	10	9	10	7	2.5	2
16	0	−4	−4	7	7	10	9	9	9	4	2	−2
17	0	−5	−4	5	9	10	10.5	9	8	7	2.5	−3.5
18	0	−4.5	4	6	9	8	10.5	9	9	2	4	−4.5
19	−2	0	4	5.5	7	10	10	10	9	2	5	−5
20	−4	1	5	5.5	7	10	9.5	9	6	−1	2	−3
21	−2	5	4.5	5	7	6	10	9	9	1	1	−2
22	−3	1	5	6	7	10	9	10	8	−3	1.5	−5
23	3	2	4	5.5	8	9	11	9	9	1	3.5	−6
24	−2.5	1	4	6	7	10	11	10	9	0	4.5	−7
25	−2	−1	6	5	10	6	11.5	9	10	1	6	−7
25	−1	−2	6	5	10	10	11	9	10	3	5.5	−5
27	−3	−1.5	9	5.5	7	6	10.5	10	9	4	6.5	−11
28	−2	−2.5	5	6	5	11	11	10	10	4	2	−10
29	−1		7	6	5	8	11.5	9.5	10	3	2	−3
30	0		5	5.5	9	8	10	9	10	4	3.5	−2
31	−4		5.5		9		10	10		4		0

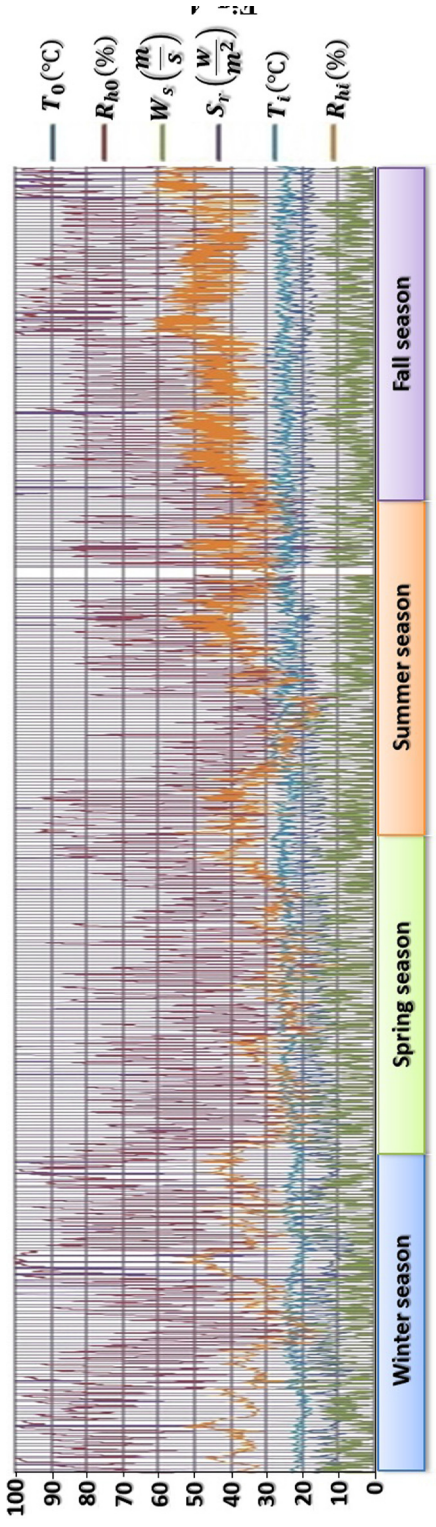

Fig. 4. The graph for the spring, summer, autumn and winter seasons that shows the data-time series.

that assigns these values is called inclusion or a membership function. In computational efficiency for complex problems, with many linguistic variables or many rules, it is fundamental to select methods that do not require many calculations or memory, so triangular or trapezoidal inclusion functions are preferable. A triangular function is commonly used in fuzzy systems as simple way to define a fuzzy set with little data and calculate the value of belonging with calculations defined by Eq. (8), the limits shown in Fig. 5, where it limits the functional limits shown that this function is suitable for modeling properties with a value of including non-zero values narrow range around the point c where the function of belonging of the group is maximum.

$$T(\mu,a,c,e)=\begin{cases}0 & \mu<a\\ \left(\frac{\mu-a}{c-a}\right) & a\leqslant\mu\leqslant c\\ \left(\frac{e-\mu}{e-c}\right) & c\leqslant\mu\leqslant e\\ 0 & \mu>e\end{cases} \tag{8}$$

The rules of fuzzy logic combine fuzzy sets of input, which are called premises, and associate a set of fuzzy output, called consequence. The rules are represented as a table for fuzzy associative memory (FAM) and is the consequence of each rule defined for each combination of two inputs, the FAM allow to make a graphical representation of the relationships between two input variables and the output variable. The next step is to associate these sets with a number of triangular partitions. It is common to use five triangular partitions, which in this case are called: Very Low [VL], Low [L], Normal [N], High [H] and Very High [VH]. The fuzzifier establishes a relationship between the non-fuzzy entry points to the system and their corresponding fuzzy sets*G*. The grouping fuzzy logical relationships by determining fuzzy logical relationships having the same left-hand side and calculate G_i for each i-th fuzzy logical relationship group is described by the Eq. (9), where μ_i is the membership function of the i-th fuzzy group.

$$G_i=\begin{bmatrix}G_1\\G_2\\G_3\\G_4\\G_5\end{bmatrix}=\begin{bmatrix}1/\mu_1 & 0.5/\mu_2 & 0/\mu_3 & 0/\mu_4 & 0/\mu_5\\ 0.5/\mu_1 & 1/\mu_2 & 0.5/\mu_3 & 0/\mu_4 & 0/\mu_5\\ 0/\mu_1 & 0.5/\mu_2 & 1/\mu_3 & 0.5/\mu_4 & 0/\mu_5\\ 0/\mu_1 & 0/\mu_2 & 0.5/\mu_3 & 1/\mu_4 & 0.5/\mu_5\\ 0/\mu_1 & 0/\mu_2 & 0/\mu_3 & 0.5/\mu_4 & 1/\mu_5\end{bmatrix} \tag{9}$$

The defuzzifier is the function that transforms a fuzzy set into a non-fuzzy output value using a fuzzy inference device. The process of defuzzification uses the centroid of the area described by the union of fuzzy sets, and is described by the area under the generating for the geometry union (A) through the Eq. (10) and the area centroid (C) calculated by the Eq. (11), where six pairs of points (x_i,μ_i) generated the geometric figure generated by the intersection of two fuzzy sets and x is the variable to be described by logic.

$$A=\frac{1}{2}\sum_{i=0}^{5}\left(x_i\mu_{i+1}-x_{i+1}\mu_i\right) \tag{10}$$

$$C=\frac{1}{6A}\sum_{i=0}^{5}\left((x_i+x_{i+1})\left(x_i\mu_{i+1}-x_{i+1}\mu_i\right)\right) \tag{11}$$

4. Results

4.1. Field measurements and ANN station models

The greenhouse has a 1 cm thick plastic layer on top. The data selected for the development of this research were: outside air temperature °C (S_1), outside air relative humidity % (S_2), wind speed m/s (S_3), and global solar radiation flux W/m^2 (S_4). Hence,

Table 2
Hidden layer matrix for artificial neural network, called changed parameters of ANN in different months of the year.

		Synaptic weights				
		$\omega_1(R_{hi})$	$\omega_2(W_s)$	$\omega_3(S_r)$	$\omega_4(T_o)$	$\omega_5(R_{ho})$
Month	1	0.94256	−0.310689	−0.0548145	0.250923	2.52923
	2	0.948636	−0.28275	0.0464792	−0.0545413	0.4914
	3	1.09808	−0.339832	0.0187778	−0.103153	−2.8627
	4	0.673155	−0.26256	0.0323826	0.27199	0.304716
	5	0.562815	−0.226705	−0.184886	0.133545	−0.584523
	6	0.193755	0.0454557	0.0734149	0.131425	0.490419
	7	0.65911	−0.188655	−0.0727979	−0.072996	−0.0865882
	8	0.904371	−0.199594	−0.144021	0.103324	0.01631
	9	0.887349	−0.234471	−0.0234992	−0.15011	0.0667453
	10	0.667061	−0.193048	−0.176446	−0.00353592	−0.47418
	11	0.697842	−0.0973856	−0.0651743	−0.717656	−4.33875
	12	0.983983	−0.285975	−0.0638287	0.0742819	7.01234

to specific time and day, this weather station is set up to analyze the sampling information every 10 min. The variables plotted are: external temperature, external humidity, wind speed, solar radiation, internal temperature and internal humidity. To obtain the coefficients of both ANN mathematical models, several measurements were taken to predict the interior air temperature in the greenhouse. This research is based on the analysis of the input variables, which are: $T_o, R_{ho}, W_s, S_r, R_{hi}$, being the inside air temperature the output variableT_i. The measurements of the previous variables were made by sampling every 10 min during a period of 365 days. They were divided into four groups, representing the four seasons of the year, although only two stations were used as data for this project: the summer and winter seasons. Thinking about the recorded Input-output values along with the performance of the experimental identification, it could be all the input signals and the desired restrictions needed during the procedure. Taking into account a group of ANN models, the correct candidate is chosen to make the best predictions in the summer and winter seasons, making a comparison to select the best model to predict the internal temperature between the real data provided with ANN models by Summer and Winter seasons as shown in Fig. 6, respectively. The percentage of data that was used for training

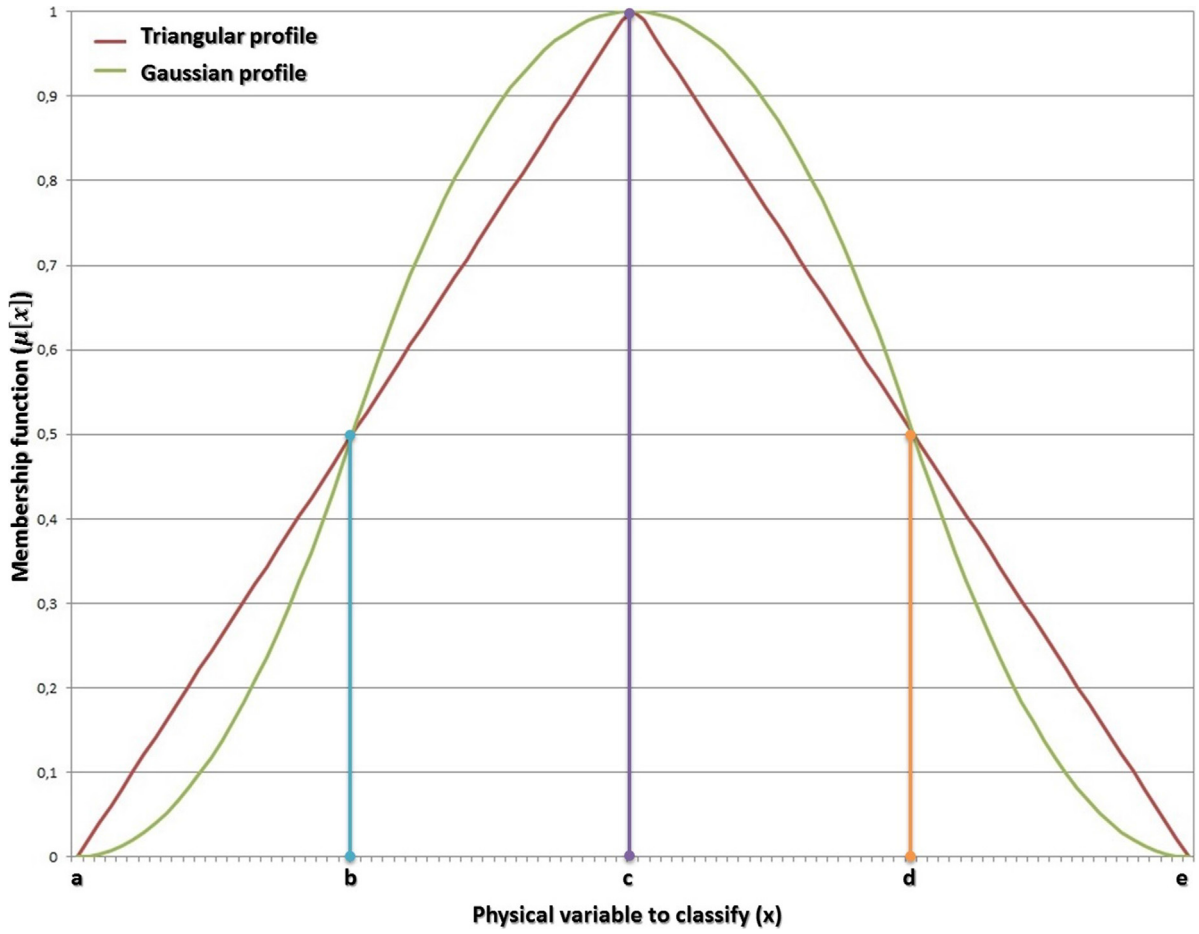

Fig. 5. Graphical representation of the Gaussian and triangular functions for variable fuzzy value belonging.

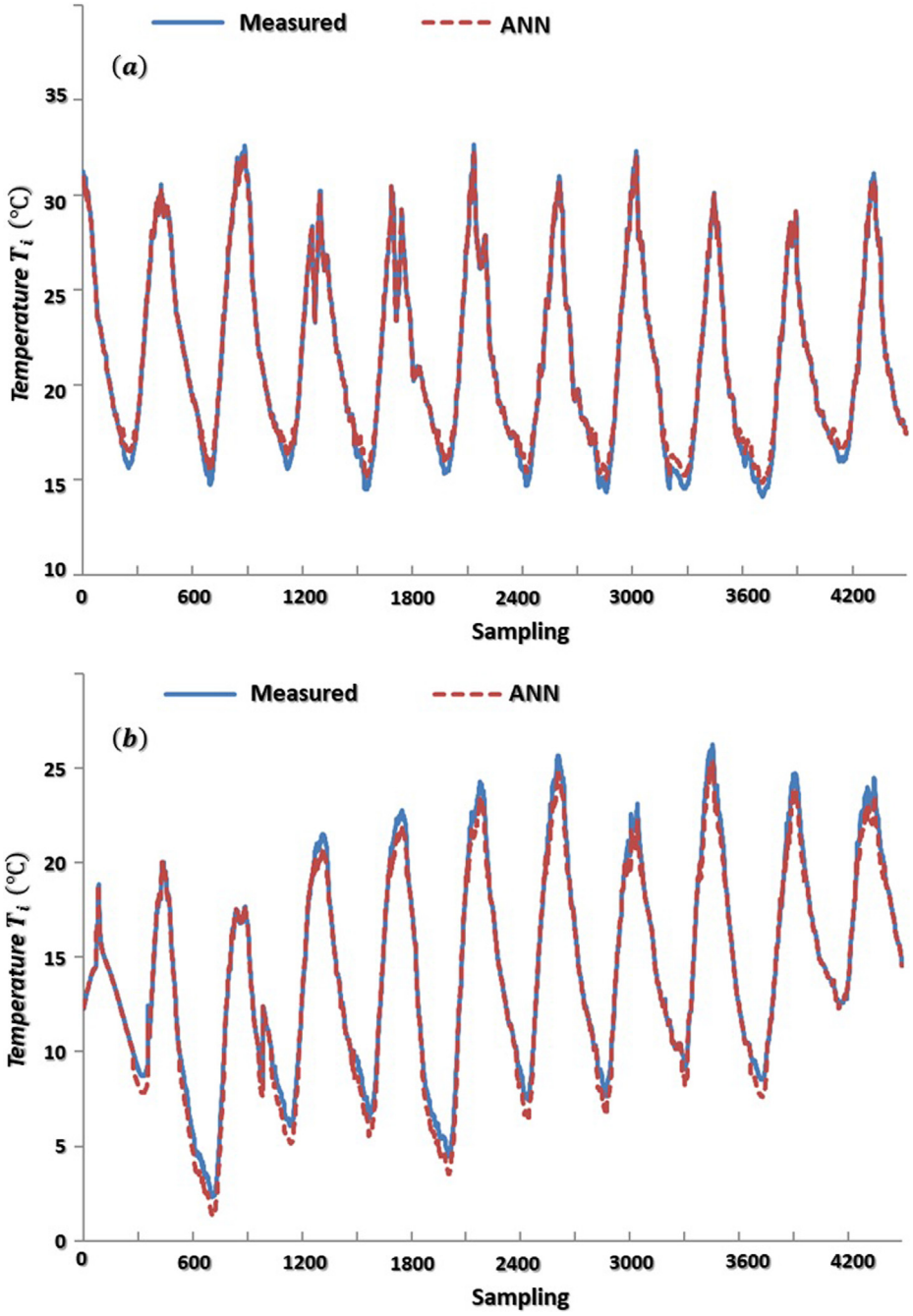

Fig. 6. Original data vs. results of the (a) artificial neural network for the summer season (b) artificial neural network for the winter season. —— Measured; - - - ANN.

and testing is approximately 50%, which corresponds to the summer and winter seasons.

4.2. Accuracy measurements

A comparison made between ANN models in different months introducing the base of the coefficient of determination (R^2), which is a measure of the correlation between the observed and predicted data, are shown in Fig. 7. The values of the parameters by the method of analysis of variance (ANOVA) in different months of the year are shown in Table 3. The ANN equation of the year-adjusted model are represented mathematically as a function $f(X)$by Eq. (12), where X_1 is R_{hi} relative humidity of the inner air,X_2 is W_s wind speed, X_3 is S_r global radiation flow solar, X_4 is T_0 outdoor air temperature, X_5 is R_{h0} relative humidity of outdoor air and T_i is the temperature of the air inside the greenhouse.

$$T_i = 3.66415 - 268.671x10^{-3}R_{hi} + 56.5276x10^{-3}W_s + 0.900254x10^{-3}S_r + 736.981x10^{-3}T_o + 382.686x10^{-3}R_{ho} \quad (12)$$

From Eq. (11), since the P-value is less than 0.05, there is a statistically significant relationship between the variables with a confidence level of 95.0%, the behavior of the linear regression of annual behavior is shown in Fig. 8, where the results of adjusting a multiple linear regression model are plotted to describe the relationship between the annual internal temperature of the greenhouse and 5 independent variables.

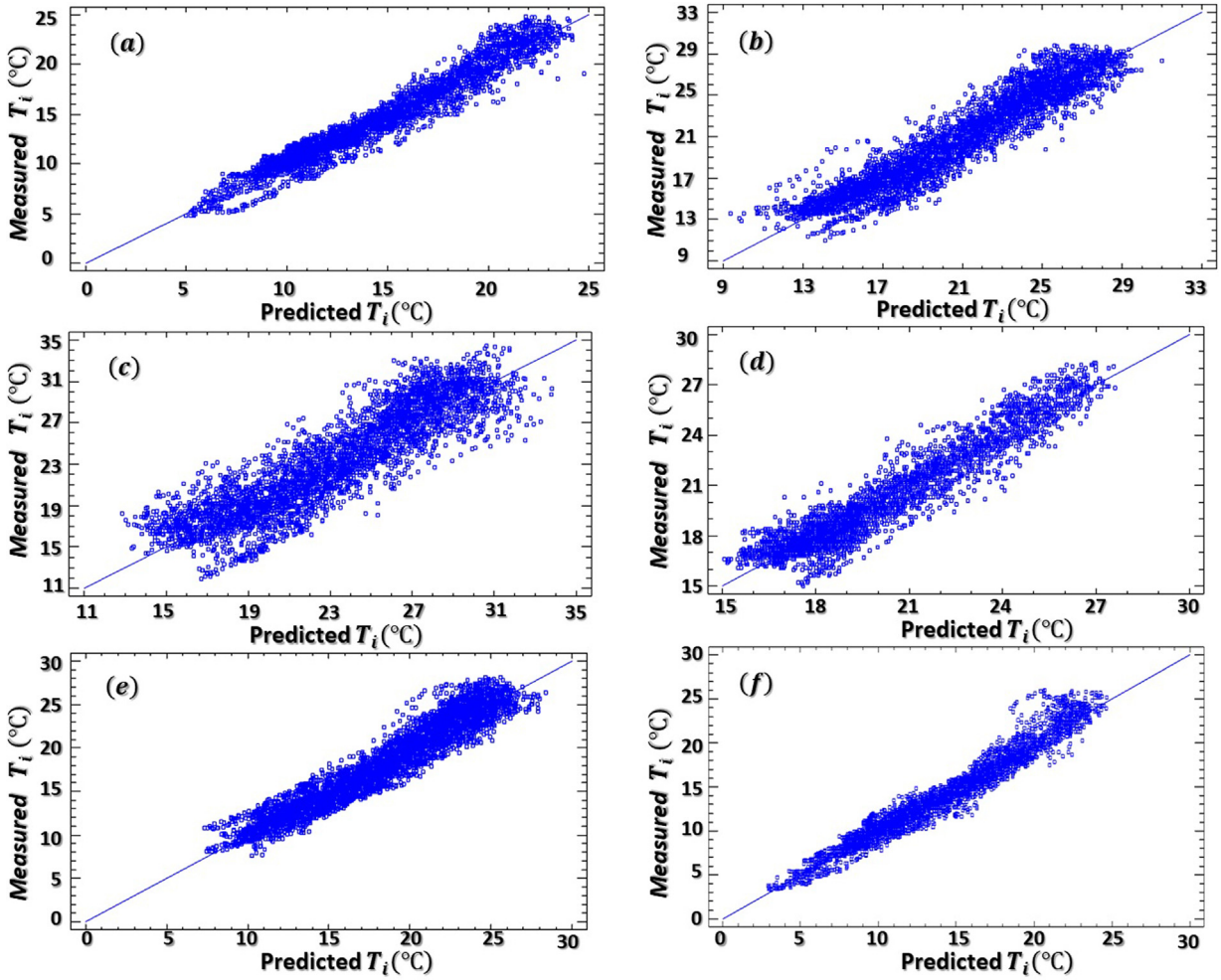

Fig. 7. Results of the multiple linear regression models for the internal greenhouse temperature in different months of the year and 5 input independent variables.

Table 3
Comparing the estimated error for the different ANN models in different months of the year.

Month	R2 (%)	Constant	R_{ho}(%)	W_s(m/s)	S_r(w/m^2)	T_o(°C)	R_{hi}(%)
January February	94.28	−1.0114	−0.236221	0.0326977	0.00059725	0.856672	0.360606
March April	90.75	28.9004	−0.187503	0.0060157	0.00148862	0.105096	0.068014
May June	89.27	7.16663	−0.24153	0.177004	0.00083953	0.565885	0.336149
July August	90.23	27.1952	−0.207019	0.0866254	0.00189649	0.111526	0.106824
September October	91.30	2.08221	−0.277121	0.0956593	0.00055788	0.75372	0.417986
November December	95.22	−1.5295	−0.240119	0.0103814	0.00106435	0.886823	0.365608

4.3. Water mechanical properties against environmental temperature

The temperatures of the semi-arid regions generally have their lowest point at higher altitudes (2000 m above sea level), whereas the water melting point is 0 °C and the water boiling point is 100 °C. It is important to consider the variation of temperature with respect to dynamic and kinematic viscosity, which is shown in Fig. 9. Mathematically, the response of kinetic and dynamic viscosity is a decreasing exposition with respect to the temperature. This response is represented by Eq. (13) and Eq. (14) respectively. The reference of some numerical values used for this physical model is described by Table 4.

$$\mu(T) = 1.81 \cdot e^{-0.0184 \cdot T} \times 10^{-4} \tag{13}$$

$$\gamma(T) = 1.78 \cdot e^{-0.018 \cdot T} \times 10^{-6} \tag{14}$$

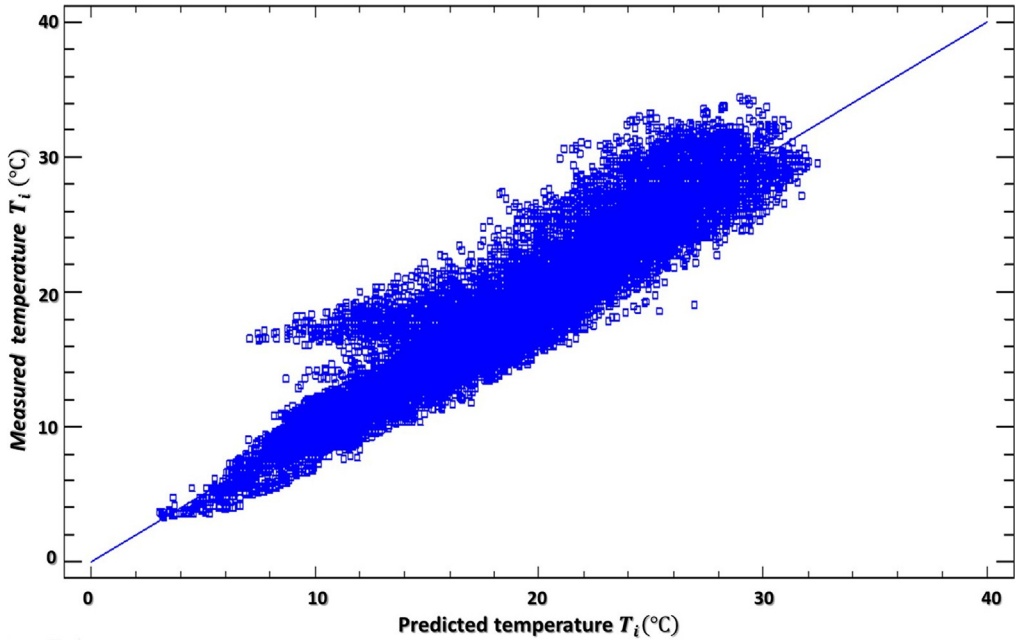

Fig. 8. Results of the multiple linear regression model between the annual internal temperature of the greenhouse and 5 input independent variables.

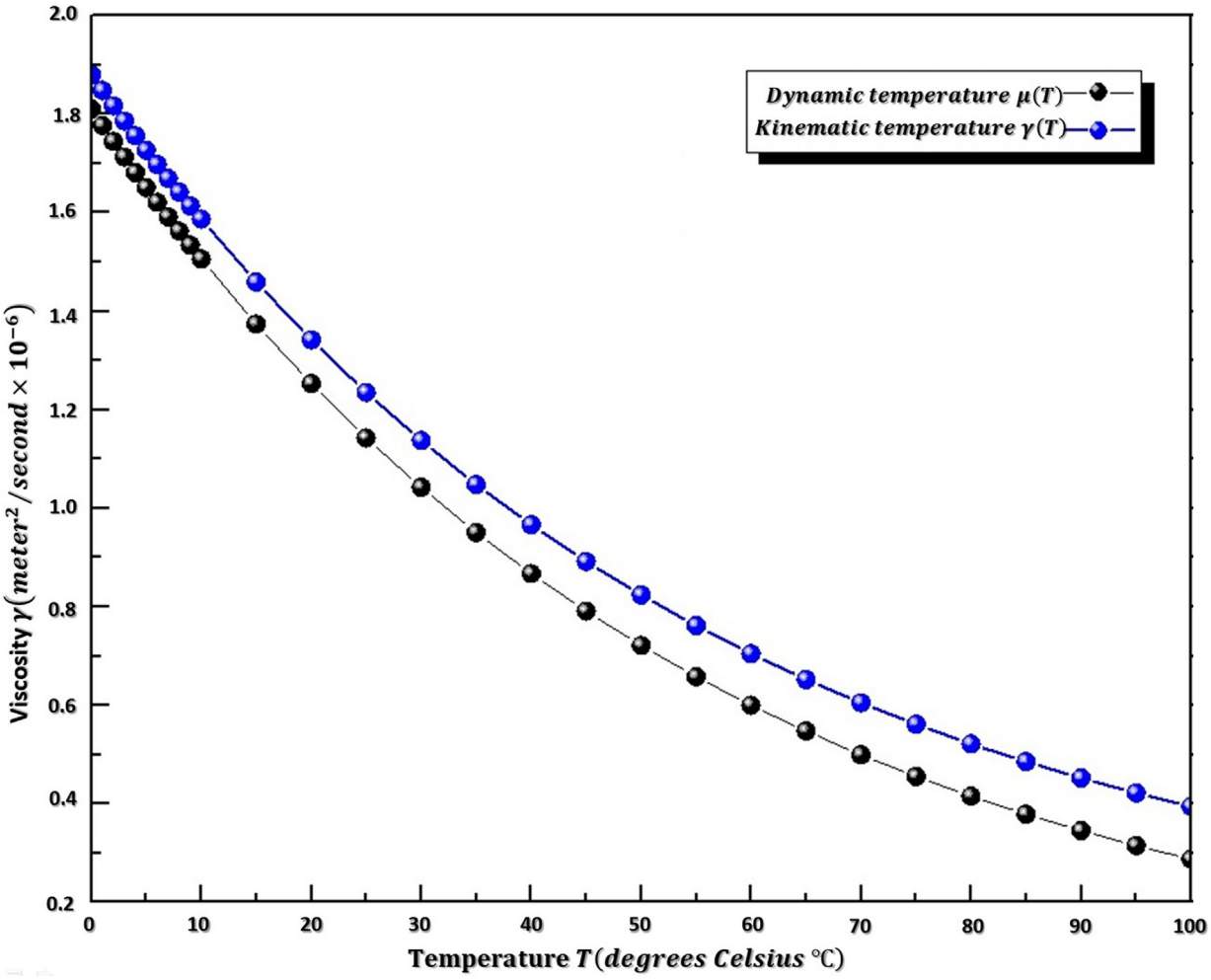

Fig. 9. Chart for the behavior of water dynamic and kinematic viscosity vs. temperature.

Table 4
Water properties for temperature vs. dynamic and kinematic viscosities.

Environmental temperatura (°C)	Water mechanical properties	
	Dynamic viscosity $(kg \cdot s/m^2) \times 10^{-4}$	Kinematic viscosity $(m^2/s) \times 10^{-6}$
0	1.7920000	1.7870000
1	1.7770005	1.7482466
2	1.7446026	1.7170597
3	1.7127955	1.6864291
4	1.6815682	1.6563449
5	1.6509103	1.6267975
6	1.6208113	1.5977771
7	1.5912611	1.5692744
8	1.5622496	1.5412801
9	1.5337670	1.5137853
10	1.5058038	1.4867809
15	1.3734514	1.3588155
20	1.2527321	1.2418638
25	1.1426234	1.1349781
30	1.0421926	1.0372918
35	0.9505893	0.9480134
40	0.8670374	0.8664190
45	0.7908292	0.7918473
50	0.7213194	0.7236939
55	0.6579192	0.6614065
60	0.6000914	0.6044800
65	0.5473465	0.5524531
70	0.4992375	0.5049041
75	0.4553571	0.4614476
80	0.4153336	0.4217314
85	0.3788279	0.3854334
90	0.3455309	0.3522596
95	0.3151605	0.3219411
100	0.2874595	0.2942320

Table 5
Fuzzy rules accurate for ecological anti-disaster system with frost irrigation in greenhouses.

The defuzzifier frost irrigation	Output activation of PWM (%)	Average temperature ranges (°C)
No frost (NF)	0–10	4
Possible frost (PF)	5–30	2
Mild frost (MF)	25–50	0
Severe frost (SF)	45–80	−2
Hard frost (HF)	75–100	−4

From the Fig. 9, the water condensation process is defined by the difference in density between cold and warm water. This feature, that in the presence frost to forming a plasticized igloo on the greenhouse surface. Therefore, these physical properties of water are exploited through the water distribution system for anti-frost preventing the cooling of the croplands through the water surface solidification (freezing of water surface), because the rate of change in the water density does not vary constantly with changes in temperature inside the greenhouse, keeping a different internal temperature (usually warmer than the outside environmental temperature) inside the frozen plastic surface despite the low temperature that occurs externally to the plastic surface of the greenhouse.

4.4. Fuzzy associative memory of ecological anti-disaster frost irrigation

Finally, the physical properties of the water and the plastic envelope of the greenhouse are exploited through a diffuse system

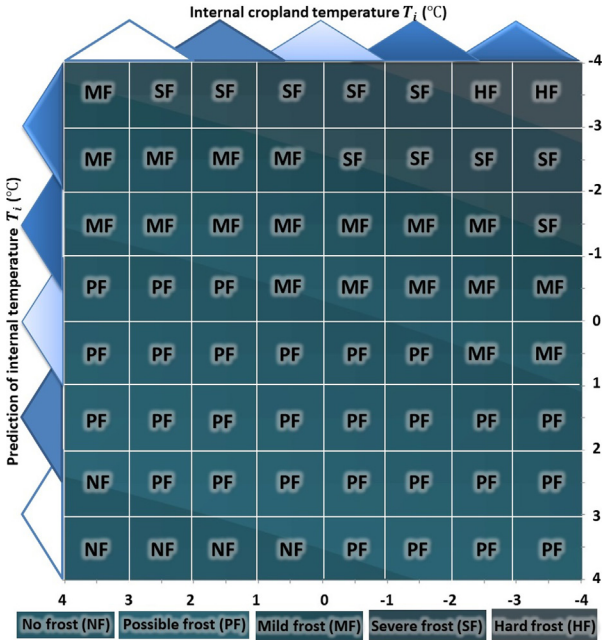

Fig. 10. Graph showing diffuse output of anti-frost irrigation system (% PWM) for cropland temperature (°C) vs. the prediction of internal temperature in the greenhouse (°C).

for smart weather station ecological anti-disaster frost irrigation. The implementation of ecological anti-disaster frost irrigation considers partitions of the input and output linguistic variables as the basis of the fuzzy rules, which depends on the method of blurring, inference and debriefing using aspects related to efficiency and adaptation. The fuzzy rules accuracy using Eq. (9), are shown in Table 5 and the results are mapped in Fig. 10, where it is classified into 5 probable states of output depending on the cropland temperature and the internal temperature of the greenhouse that is predicted by the ANN, classified as: Hard-Freeze (HF), Severe-Freeze (SF), Soft-Freeze (MF), Possible-Frost (PF), No-Frost (NF). For the activation of the water pump system for the ecological anti-disaster frost irrigation, a technique is used for percentage activation energy called Pulse Width Modulation (PWM). Hence, the PWM allows having a 0% off state and when it is required to the maximum of its power is 100%. Consequently, this activation percentage for presence of the frost is assigned through Fuzzy Associative Memory (FAM). Moreover, this percentage assigned is shown in Table 6, where the data used for shaping the fuzzy map are shown. Additionally, the results of the fuzzy rules accuracy and the values to output activation of PWM (%) for the defuzzifier frost irrigation are shown in Fig. 11. Finally, the fuzzy frost actions are classified in: the state of No Frost (NF) corresponding at 0–10% PWM activation for an average temperature of 4 °C, the state of Possible Frost (PF) corresponding at 5–30% PWM activation for an average temperature of 2 °C, the state of Mild Frost (MF) corresponding at 25–50% PWM activation for an average temperature of 0 °C, the state of Severe Frost (SF) corresponding at 45–80% PWM activation for an average temperature of −2 °C and finally, the state of Hard Frost (HF) corresponding at 75–100% PWM activation for an average temperature of −4 °C.

5. Conclusions and future works

In this paper we developed an intelligent system for environmental application through a fuzzy water pump system and smart

Table 6
Values table for fuzzy associative memory (FAM) and the relationships between two input variables and the output variable (% PWM).

		Predicted ANN temperature (°C)								
		4	3	2	1	0	−1	−2	−3	−4
Cropland temperature (°C)	4	15.0	15.7	16.5	17.4	18.4	19.5	20.7	22.1	23.7
	3	17.9	18.8	19.8	20.8	22.0	23.3	24.8	26.4	28.4
	2	21.5	22.5	23.7	24.9	26.3	27.9	29.7	31.7	34.0
	1	25.7	27.0	28.3	29.8	31.5	33.4	35.5	37.9	40.7
	0	30.8	32.3	33.9	35.7	37.7	40.0	42.5	45.4	48.7
	−1	36.9	38.6	40.6	42.8	45.2	47.9	50.9	54.3	58.3
	−2	44.1	46.3	48.6	51.2	54.1	57.3	60.9	65.0	69.8
	−3	52.8	55.4	58.2	61.3	64.7	68.6	72.9	77.9	83.5
	−4	63.3	66.3	69.7	73.4	77.5	82.1	87.3	93.2	100.0

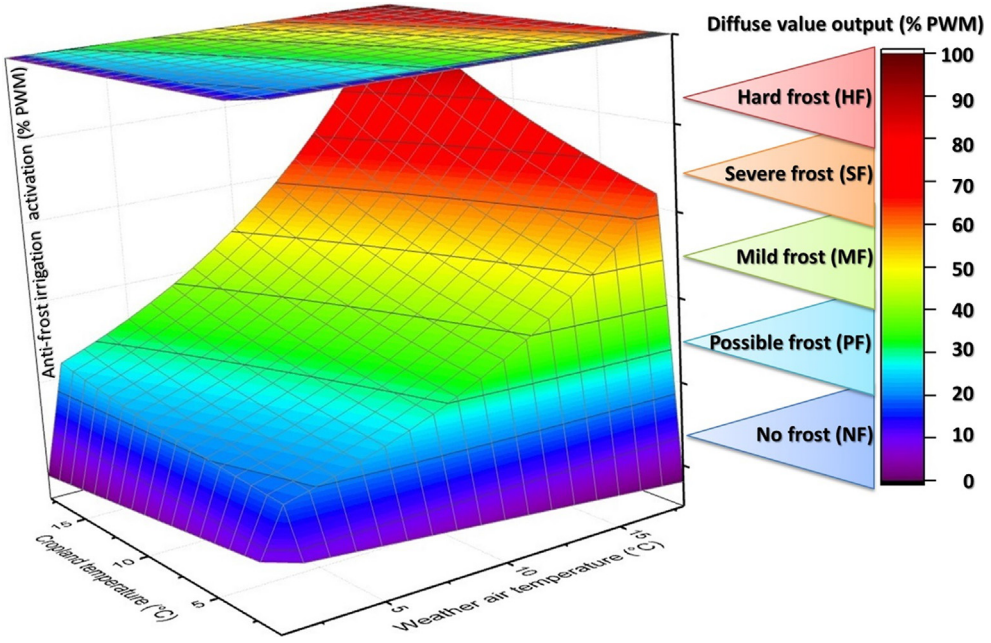

Fig. 11. Fuzzy associative memory (FAM) and the relationships between cropland temperature (°C) and predicted ANN temperature (°C) input variables and the ecological anti-disaster frost irrigation (% PWM) output variable.

weather station for the ecological anti-disaster frost irrigation. These artificial intelligence techniques can be applied to a smart farming system that can be performed through the internet of things (IoT) in environmental applications. Additionally, the method developed allows to estimate the desired parameter of the Pulse Width Modulation (PWM) output that can be used for the anti-frost irrigation control in greenhouses. According to its application, in the smart frost control on greenhouses, we proposed the use of linear autoregressive models with models of external ANN to predict the dynamic behavior of air temperature inside a greenhouse. The temperature predictor uses an ANN of multilayer Perceptron (MLP), which is trained by backward propagation algorithm (BPA), and the validity of the data was made by analysis of variance (ANOVA). Hence, this feature improved upon the prediction. Therefore, measurements of the outside air temperature, the relative humidity of the outside air, the wind speed, the global solar radiation flow, the relative humidity of the indoor air were used as input variables to the system and were tested different structures of the ANN model. The external climatic variables provided by the meteorological station were divided into two main sections corresponding to the summer and winter seasons, in order to develop and evaluate the ANN model and the data sample. Additionally, through programming means, the performance indices for each of the structures were calculated, selecting those models with better prediction of the real conditions of the interior temperature. The ANOVA statistical method was used to analyze the variation of the two seasons comparing the neural network and the results of the ANN models in different months of the year compared with the real data. The best results of the prediction of the interior temperature were obtained by the structures of the ANN models; with a confidence level of 95%. The intelligent forecasting application uses the fuzzy classification system with a triangular profile which adjusts to the presence of frost. We implemented a fuzzy logic system for the classification of the water pump system for the ecological irrigation anti-disaster by freezing, where a diffuse associative memory (FAM) was applied, which is classified as: Hard-Freeze (HF) from 100 to 80 percent probability, Severe-Freeze (SF) from 80 to 60 percent probability, Soft-Freeze (MF) from 60 to 40 percent probability, Possible-Frost (PF) from 40 to 20 percent probability, No-Frost (NF) from 20 to 0 percent probability, respectively. Results of the FAM use the relationships between cropland temperature (°C) and predicted ANN temperature (°C) input variables for activation of ecological anti-disaster frost irrigation (% PWM) in 5 probability states and graduates every 20 percent probability. The technological innovation applied to smart farming and frost intelligent control in applications of extreme

environmental microclimate is the activation of the output variable for ecological irrigation anti-disaster by freezing (% PWM), which transforms the greenhouse into an igloo. The Internet of Things (IoT) in environmental applications is developed through the use of a web page and cellular technology (GSM/GPRS) through a Wireless Application Protocol (WAP), which is a technical standard for accessing information through a mobile wireless network. Moreover, the implementation for smart alerts and notifications to be useful in farming that exposed to environmental freezing through digital innovation.

Declaration of Competing Interest

The authors declare that they have no known competing financial interests or personal relationships that could have appeared to influence the work reported in this paper.

Acknowledgements

The authors wish to thank Rene Preza-Cortés of Applied Physics and Advanced Technology Center UNAM for their technical support. The financial support of CONACYT Mexican mixed funds of the Zacatecas State Government (COZCyT) through ZAC-2009-C01-121774 project and the Queretaro State Government (CONCYTEQ) through QRO-2005-C01-15218 project is also, gratefully acknowledged.

References

[1] Z. Azaizia, S. Kooli, I. Hamdi, W. Elkhal, A.A. Guizani, Experimental study of a new mixed mode solar greenhouse drying system with and without thermal energy storage for pepper, Renew. Energy 145 (2020) 1972–1984, https://doi.org/10.1016/j.renene.2019.07.055.

[2] A. Castañeda-Miranda, M. Icaza, V.M. Castaño, Meteorological temperature and humidity prediction from Fourier-statistical analysis of hourly data, Adv. Meteorol. (2019) 13, https://doi.org/10.1155/2019/4164097, Article ID 4164097.

[3] A. Castañeda-Miranda, V.M. Castaño, Smart frost control in greenhouses by neural networks models, Comput. Electron. Agric. 137 (2017) 102–114, https://doi.org/10.1016/j.compag.2017.03.024.

[4] I. Charania, X. Li, Smart farming: agriculture's shift from a labor intensive to technology native industry, Internet of Things 9 (2020), https://doi.org/10.1016/j.iot.2019.100142 100142.

[5] C. Chen, F. Han, K. Mahkamov, S. Wei, X. Ma, H. Ling, C. Zhao, Numerical and experimental study of laboratory and full-scale prototypes of the novel solar multi-surface air collector with double-receiver tubes integrated into a greenhouse heating system, Sol. Energy 202 (2020) 86–103, https://doi.org/10.1016/j.solener.2020.03.063.

[6] N. Choab, A. Allouhi, A. El Maakoul, T. Kousksou, S. Saadeddine, A. Jamil, Review on greenhouse microclimate and application: design parameters, thermal modeling and simulation, climate controlling technologies, Sol. Energy 191 (2019) 109–137, https://doi.org/10.1016/j.solener.2019.08.042.

[7] Y.J. Cui, K.F. Wang, J.E. Li, B.L. Wang, Time-dependent power output and elastic/plastic fracture analyses of porous thermoelectric ceramics for generators, Ceram. Int. 46 (6) (2020) 8264–8273, https://doi.org/10.1016/j.ceramint.2019.12.055.

[8] V.W.J. van Heusinkveld, J.A. Hooft, B. Schilperoort, P. Baas, M. ten Veldhuis, B. van de Wiel, Towards a physics-based understanding of fruit frost protection using wind machines, Agric. For. Meteorol. 282–283 (2020), https://doi.org/10.1016/j.agrformet.2019.107868 107868.

[9] S. Huang, Y. Ye, X. Cui, A. Cheng, G. Liu, Theoretical and experimental study of the frost heaving characteristics of the saturated sandstone under low temperature, Cold Reg. Sci. Technol. 174 (2020), https://doi.org/10.1016/j.coldregions.2020.103036 103036.

[10] E. Iddio, L. Wang, Y. Thomas, G. McMorrow, A. Denzer, Energy efficient operation and modeling for greenhouses: a literature review, Renew. Sustain. Energy Rev. 117 (2020), https://doi.org/10.1016/j.rser.2019.109480 109480.

[11] A. Khanlari, A. Sözen, C. Şirin, A.D. Tuncer, A. Gungor, Performance enhancement of a greenhouse dryer: analysis of a cost-effective alternative solar air heater, J. Cleaner Prod. 251 (2020), https://doi.org/10.1016/j.jclepro.2019.119672 119672.

[12] M.P. Lebedev, O.V. Startsev, A.K. Kychkin, The effects of aggressive environments on the mechanical properties of basalt plastics, Heliyon 6 (3) (2020), https://doi.org/10.1016/j.heliyon.2020.e03481 e03481.

[13] G. Li, N. Li, Y. Bai, N. Liu, M. He, M. Yang, A novel simple practical thermal-hydraulic-mechanical (THM) coupling model with water-ice phase change, Comput. Geotech. 118 (2020), https://doi.org/10.1016/j.compgeo.2019.103357 103357.

[14] E. Liu, Y. Lai, Thermo-poromechanics-based viscoplastic damage constitutive model for saturated frozen soil, Int. J. Plast. 128 (2020), https://doi.org/10.1016/j.ijplas.2020.102683 102683.

[15] D. Ma, N. Carpenter, H. Maki, T.U. Rehman, M.R. Tuinstra, J. Jin, Greenhouse environment modeling and simulation for microclimate control, Comput. Electron. Agric. 162 (2019) 134–142, https://doi.org/10.1016/j.compag.2019.04.013.

[16] G. Maydana, M. Romagnoli, M. Cunha, M. Portapila, Integrated valuation of alternative land use scenarios in the agricultural ecosystem of a watershed with limited available data, in the Pampas region of Argentina, Sci. Total Environ. 714 (2020), https://doi.org/10.1016/j.scitotenv.2019.136430 136430.

[17] M. Mohsenipour, M. Ebadollahi, H. Rostamzadeh, M. Amidpour, Design and evaluation of a solar-based trigeneration system for a nearly zero energy greenhouse in arid region, J. Cleaner Prod. 254 (2020), https://doi.org/10.1016/j.jclepro.2020.119990 119990.

[18] M. Monika, P. Piotr, S. Marcin, G. Altantsetseg, M. Suska, Plant response to N availability in permafrost-affected alpine wetlands in arid and semi-arid climate zones, Sci. Total Environ. 721 (2020), https://doi.org/10.1016/j.scitotenv.2020.137791 137791.

[19] G. Neuner, B. Huber, A. Plangger, J.M. Pohlin, J. Walde, Low temperatures at higher elevations require plants to exhibit increased freezing resistance throughout the summer months, Environ. Exp. Bot. 169 (2020), https://doi.org/10.1016/j.envexpbot.2019.103882 103882.

[20] G.K. Ntinas, D. Dannehl, I. Schuch, T. Rocksch, U. Schmidt, Sustainable greenhouse production with minimised carbon footprint by energy export, Biosyst. Eng. 189 (2020) 164–178, https://doi.org/10.1016/j.biosystemseng.2019.11.012.

[21] S.L. Patil, H.J. Tantau, V.M. Salokhe, Modelling of tropical greenhouse temperature by auto regressive and neural network models, Biosyst. Eng. 99 (2008) 423–431, https://doi.org/10.1016/j.biosystemseng.2007.11.009.

[22] T. Rajaee, S. Khani, M. Ravansalar, Artificial intelligence-based single and hybrid models for prediction of water quality in rivers: a review, Chemometr. Intell. Lab. Syst. 200 (2020), https://doi.org/10.1016/j.chemolab.2020.103978 103978.

[23] S. Sadowski, P. Spachos, Wireless technologies for smart agricultural monitoring using internet of things devices with energy harvesting capabilities, Comput. Electron. Agric. 172 (2020), https://doi.org/10.1016/j.compag.2020.105338 105338.

[24] Redmond R. Shamshiri, Iva Bojic, Eldert van Henten, Siva K. Balasundram, Volker Dworak, Muhammad Sultan, Cornelia Weltzien, Model-based evaluation of greenhouse microclimate using IoT-Sensor data fusion for energy efficient crop production, J. Cleaner Prod. 263 (2020) 121303, https://doi.org/10.1016/j.jclepro.2020.121303.

[25] H. Uchida, G. Pieters, M. Deltour, Modelling greenhouse temperature by means of auto regressive models, Biosyst. Eng. 84 (2003) 147–157, https://doi.org/10.1016/S1537-5110(02)00239-8.

[26] P. Valverde, M. Zucchini, S. Polverigiani, E.M. Lodolini, F.J. López, D. Neri, Olive knot damages in ten olive cultivars after late-winter frost in central Italy, Sci. Hortic. 266 (2020), https://doi.org/10.1016/j.scienta.2020.109274 109274.

[27] A. Villa, G.T.C. Edwards, L.A. Pesonen, O. Green, C.A. Grøn, Internet of Things in arable farming: Implementation, applications, challenges and potential, Biosyst. Eng. 191 (2020) 60–84, https://doi.org/10.1016/j.biosystemseng.2019.12.013.

[28] S. Wan, P. Xu, K. Wang, J. Yang, S. Li, Real-time estimation of thermal boundary of unsteady heat conduction system using PID algorithm, Int. J. Therm. Sci. 153 (2020), https://doi.org/10.1016/j.ijthermalsci.2020.106395 106395.

[29] K. Wang, E. Jafarov, I. Overeem, Sensitivity evaluation of the Kudryavtsev permafrost model, Sci. Total Environ. 720 (2020), https://doi.org/10.1016/j.scitotenv.2020.137538 137538.

[30] K. Yang, Y. Wang, Y. You, H. Yang, X. Hao, Non-equilibrium polymerization enables adhesive material with anti-freezing, multipurpose adhesion, long-term air stability and anisotropic deformation, Chem. Eng. J. 382 (2020), https://doi.org/10.1016/j.cej.2019.122926 122926.

[31] A. Zendehboudi, S.H. Hosseini, G. Ahmadi, Modeling of frost thermal conductivity on parallel surface channels, Measurement 140 (2019) 293–304, https://doi.org/10.1016/j.measurement.2019.03.045.

[32] F. Prado, M. Minutolo, W. Kristjanpoller, Forecasting based on an ensemble Autoregressive Moving Average - Adaptive neuro - Fuzzy inference system – Neural network - Genetic Algorithm Framework, Energy 197 (2020), https://doi.org/10.1016/j.energy.2020.117159 117159.

[33] X. Zhao, G. Zhou, X. Jiang, Measurement of thermal conductivity for frozen soil at temperatures close to 0 °C, Measurement 140 (2019) 504–510, https://doi.org/10.1016/j.measurement.2019.03.069.